Quantifying Crystalline Fraction within Polymer Spherulites

Konstantinos G. Gatos,[†,‡] Chrysa Minogianni,[†,‡] and Costas Galiotis*[,†,‡,§]

Institute of Chemical Engineering and High Temperature Chemical Processes, Foundation for Research and Technology—Hellas (FORTH/ICE-HT), P.O. Box 1414, Patras 26504, Greece; Inter-Departmental Programme of Graduate Studies in Polymer Science and Technology, University of Patras, Greece; and Department of Materials Science, University of Patras, 26500 Patras, Greece

Received October 9, 2006
Revised Manuscript Received December 5, 2006

Spherulites are polycrystalline structures and can be found in a variety of natural solids such as metals[1] and rocks[2] but also in synthetic materials such as polymers.[3] Back in the 19th century Lehmann[4] described the spherulites as spherical aggregates being comprised of fibrillar crystal arrays radiating from a common central nucleus. In spite of their technological importance particularly for engineering plastics, a unique description of their formation and growth is not as yet complete.[3] In polymers the spherulites themselves are semicrystalline structures that consist of single-crystal lamellae and interlamellar amorphous matter. Although the relative proportion of the two phases within the spherulite can be altered by material factors such as the molecular weight and/or crystallization conditions, there is no technique available to date that can yield quantitative information on the crystalline fraction within the spherulite at the microscale. Polypropylene, for example, is a semicrystalline thermoplastic that finds wide use in a variety of applications.[5] Key aspects of its performance regarding solvent penetration,[5] vapor transport,[6] and mechanical strength[7] are greatly affected by the degree of crystallinity. Needless to say, the size of the spherulites obtained during crystallization in the melt[3,8] and the intrinsic interplay of the crystalline and amorphous moieties are factors of great significance.[3]

Crystallizable polypropylene can be produced in two distinct stereoisomers, namely isotactic (iPP) and syndiotactic (sPP). iPP, itself, crystallizes in four distinct forms (α, β, γ, and δ) depending upon cooling conditions and additives. The most frequently crystal modification obtained is the monoclinic α form.[9] The β form is thermodynamically less stable and is crystallized into a hexagonal unit cell.[10,11] For low molecular weight iPP or under crystallization at elevated pressures the γ form[12] of triclinic symmetry unit cell can be obtained. The δ form refers to a pseudo-hexagonal unit structure (smectic form)[13] and is produced at high cooling rates. The α form of iPP has a high tendency to build spherulites upon crystallization in the melt. The growth and interplay of these regions are directly related to the crystalline volume in the interior of the spherulite and thus with the overall degree of crystallinity.

As presented recently,[14] laser Raman spectroscopy (LRS) can be used to evaluate the crystallinity in iPP, exploiting the vibrational peaks in the region of 750−880 cm^{-1}. 3-d crystallinity can be expressed by the 809 cm^{-1} band assigned to the $\rho(CH_2)$ mode coupling with the skeletal stretching mode, whereas all noncrystalline domains result in a primary peak at 841 cm^{-1} and two other minor peaks at 830 and 854 cm^{-1}. The 841 cm^{-1} peak corresponds to $\rho(CH_2)$ vibrations present in unoriented hydrocarbons while the other two satellite bands are assigned to short-range 3_1-helical conformations.[14] The relative integrated intensity of the 809 cm^{-1} band can be considered as an easy—nondestructive—and reliable method for the determination of degree of crystallinity, X_c, via the following equation:[14]

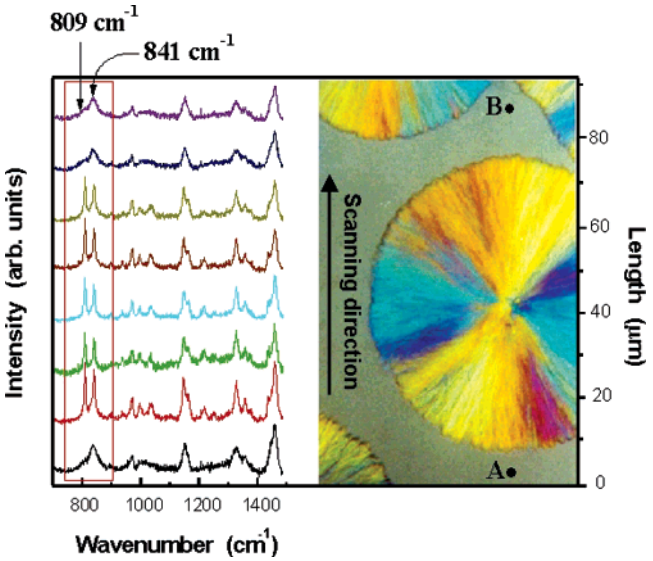

Figure 1. Raman spectra recorded along a diameter of an iPP spherulite (~80 μm in diameter) during isothermal crystallization from the melt at T_c = 130 °C. The band of interest in the region of 750−880 cm^{-1} is highlighted. Note that the path of the laser beam along the spherulite is indicated by the line connecting A to B.

$$X_c = \frac{I_{809}}{I_{809} + I_{830} + I_{841} + I_{854}} \quad (1)$$

The denominator of eq 1 has been found to be a measure of the total $\rho(CH_2)$ vibrations and is approximately constant at all crystalline fractions and the melt.[14] Since the crystalline 809 cm^{-1} appears to be a very sharp Lorentzian peak, the main source of error in estimating Raman crystallinity is the value of the denominator in eq 1, which is in turn dependent on the quality of the raw data and the goodness of the fit for all bands. For relatively small values of crystallinity near the melt the predicted error in crystallinity measurement is less than 5%. For higher crystallinities the corresponding error can be as high as 10% of measured values. As is evident, the error in crystallinity measurements does not affect the trend observed in Figure 2.

The iPP granules (INSPIRE H507-03Z supplied by Dow Chemicals) were placed between two cover slides at a thickness of about 100 μm and set on a Linkam THMS 600 hot stage. A temperature controller (Linkam TMS 93) was employed to apply the desired temperature profile. The hot stage was mounted under a modified Nikon microscope, and a long focal distance 80× microscope objective was used to focus the incident laser beam onto the specimen. The Raman spectra were taken with the 514.5 nm line of an argon ion laser and analyzed in a SPEX

* To whom all correspondence should be addressed: e-mail c.galiotis@iceht.forth.gr, fax +30 2610 965 275, tel +30 2610 965 255.
† FORTH/ICE-HT.
‡ Inter-Departmental Programme of Graduate Studies in Polymer Science and Technology, University of Patras.
§ Department of Materials Science, University of Patras.

10.1021/ma0623284 CCC: $37.00
Published on Web 01/17/2007

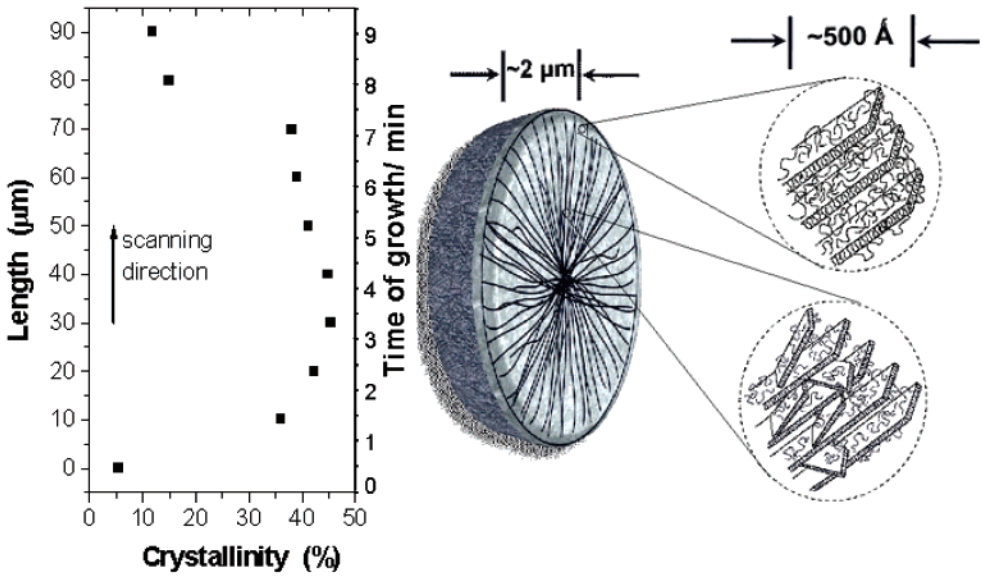

Figure 2. Crystallinity evaluation along a diameter of an iPP spherulite (~80 μm diameter size) during isothermal crystallization from the melt at T_c = 130 °C. Both scanning length and time of spherulite growth. The depicted spherulite slice of ~2 μm is related to the spatial resolution of the laser beam. The two zoomed spherulite areas correspond to its edge and interior region showing the lamellae packing.

triplemate monochromator. The iPP was taken to full melt under an inert atmosphere and then was crystallized isothermally at T_c = 130 °C. As the distance between the two cover slides glasses was ~100 μm, nucleation was induced first at the surface of the top cover slide which yielded spherulites of hemispherical shapes (facing the glass), as depicted in Figures 1 and 2. Recording of Raman spectra at steps of 10 μm was carried out when a spherulite of about 80 μm (in diameter) had been clearly grown. Raman scanning along the diameter (see Figure 3a) of the hemispherical spherulite were made at no preferred laser polarization or analysis. Hence, the effect of crystalline orientation on the integrated intensity of the Raman peaks is deemed very low. The spherulite obtained under isothermal crystallization from the melt at 130 °C is a positive radial α-spherulite type presenting clearly the pattern of the so-called "Maltese cross".[3,8] Every measurement lasted ~60 s; by the end of the experiment the spherulite had not shown any remarkable change in size.

As shown in Figure 1, the Raman spectra recorded along the diameter of an iPP spherulite were recorded between points A and B. The characteristic Raman bands (at 809 and 841 cm^{-1}) that were fully analyzed in order to obtain the crystalline fraction are also indicated in Figure 1. Their interplay is related to the degree of crystallinity,[14] and as seen in Figure 1 it varies notably as the laser beam scans along the ~80 μm spherulite diameter. At points A and B (cf. Figure 1), the weakness of the 809 cm^{-1} band indicates high amorphous content as expected also from the lack of any structure in the optical micrograph. However, as explained elsewhere,[14,15] the nomimal value of 5% obtained through the Raman technique represents statistically random conformations that can give rise to a very weak ~809 cm^{-1} band and cannot be considered as "true" crystallinity. This has indeed been taken into account when value of crystallinities are estimated on the basis of vibrational spectroscopy measurements.[14,15] The Raman spectrum recorded just as the laser beam enters the spherulite indicates an abrupt increase of crystallinity to 35% (Figure 2). Moving along the diameter of the spherulite, the crystallinity values increase further to a maximum 45% as the beam approaches the core of the spherulite. It is interesting to note that the crystallinity profile is symmetrical and peaks approximately at the spherulite nucleus. The results presented in Figure 2 have been obtained with a laser beam probe of a spatial resolution of ~2 μm. Thus, as shown schematically, the information is collected from polymer chains within an optical skin of ~2 μm and at a scanning step of 10 μm. The more dense packing of the chain-folded lamellae (magnified section in Figure 2) away from the fronts of the spherulite is usually attributed to the fibril branching at small noncrystallographic angles of the main fibril growth.[8]

The advantages of laser Raman microscopy over other techniques for the determination of the degree of crystallinity have been examined in a previous publication.[15] In short, the LRM can provide information at the molecular level in a nondestructive way at a fraction of time required by other methods. In Figure 2 the time taken for a spherulite crystallinity "snapshot" is on the order of seconds rather than minutes or hours required by other techniques. The half-time for crystallization at 130 °C as determined by microscopic observations was about 28 min, and this agrees broadly with the results obtained by Kolb et al.[16] by means of microfocus WAXS/SAXS experiments. The spherulite growth presented here was completed within ~6 min (Figure 2), whereas the sampling of one-half of the sperulite took no more than 3 min. Futhermore, no spherulite impingement was observed within the sampling time (Figure 1), and therefore, it can be safely assumed that no appreciable secondary crystallization took place. It is worth adding here, however, that the laser Raman technique is indeed ideal for the determination of secondary crystallization at long residence times. Such work is currently in progress.

In order to get a better insight into the interior of the spherulite, images from the vicinity of the spherulite center after its full growth were taken. A polarized transmission optical microscopy and an atomic force microscopy (AFM) were used (Figure 3). As shown in Figure 3a, the branching of the main fibrils creates a "hedrite-like" structure, as a subunit of the spherulite. The AFM experiment was performed in tapping mode at room temperature by means of a MultiMode scanning probe manufactured by Digital Instruments (Santa Barbara, CA). Note that no use of image filtering was employed. A microfabricated silicon cantilever with an integral tip (tapping mode tip) was employed to examine the surface topology of polymorphism after chemical etching. The etching procedure itself

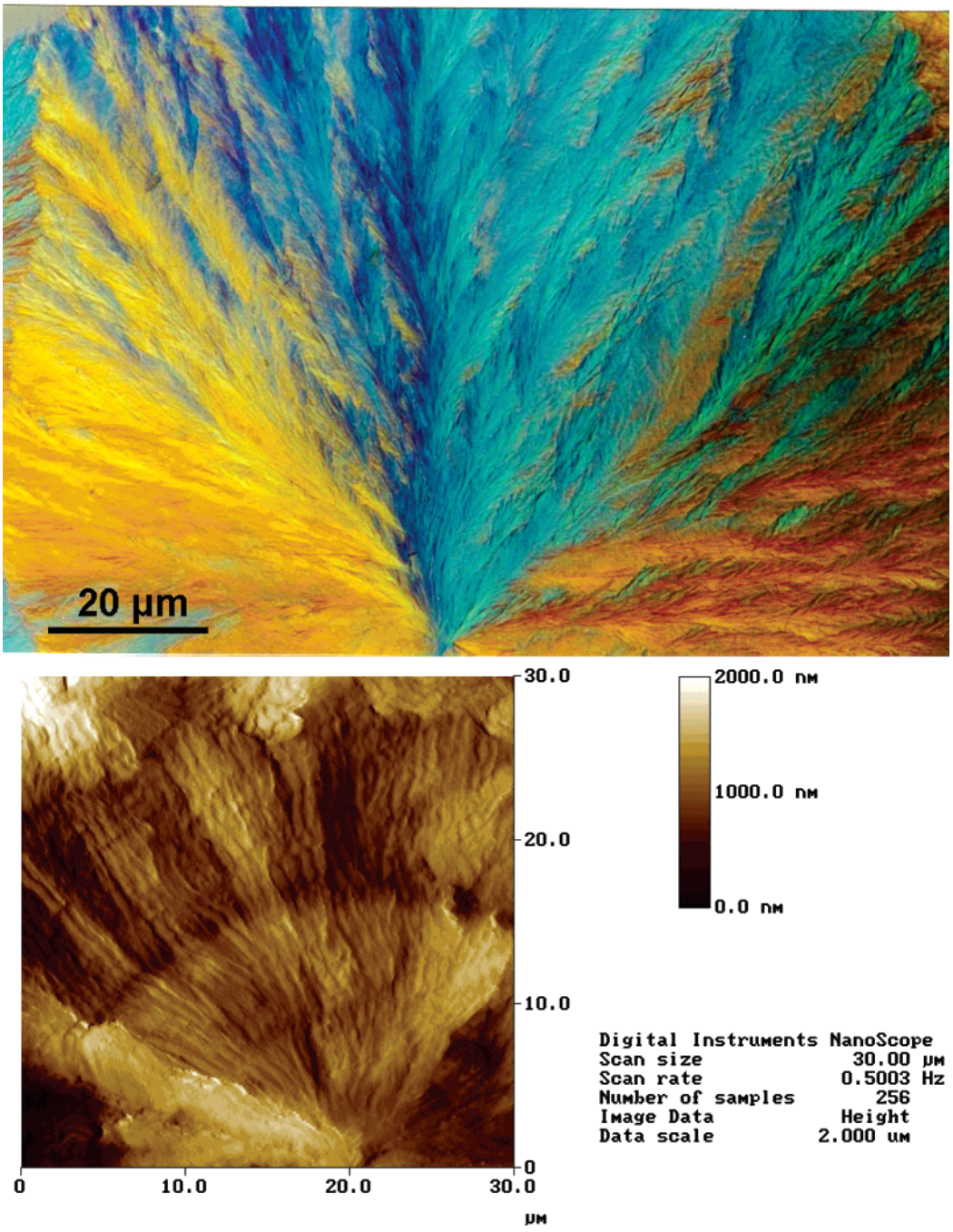

Figure 3. (a, top) Polarized transmission optical microscopic and (b, bottom) atomic force microscope (AFM) images recorded from the center of an a-iPP spherulite crystallized at 130 °C. The "mountains" and the "valleys" appeared in the AFM image after etching, corresponding to the crystalline and amorphous regions, respectively.

was conducted according to the procedure proposed earlier.[17] The lamellar organization of PP has been studied in the past, revealing essential features from the interior of PP spherulites.[18,19] In Figure 3b, the radial morphology of the iPP spherulite is evident, and the more condensed packing in the center of the structure is well resolved. The permanganic etching removed parts of the amorphous regions between the lamellae, revealing the crystalline material at the surface. It seems that the higher crystallinity values, which were obtained at the center of the spherulite (cf. Figure 2), emanate from an area of the spherulitic structure where a more condensed and folded fibril packing is present (Figure 3b).

Since, as mentioned earlier, the spherulitic structure was not fully expanded due to the constraints imposed by the proximity of the cover slides, the presented measurements correspond to sampling along the diameter of a circular "disk" that is 2 μm in thickness. As shown in both Figures 2 and 3a, the crystalline orientation along the diameter of the spherulite does not vary appreciably to affect the results reported here. Hence, one can safely assume that the variations in the relative intensities of the Raman bands are due to variations in the crystalline content rather than crystalline orientation. As expected, the crystalline profile obtained exhibits a maximum at the center of the spherulite due to the more condensed packing of the lamellae and a minimum value in regions near the circumference.

The current study attempts for the first time to obtain the crystallinity profile in the interior of a single iPP spherulite crystallized from the melt. As is evident, Raman microscopy appears to be an ideal technique for fast quantification of crystallinity at the microscale. The methodology presented here

can be further elaborated by means of Raman measurements at resolutions under the diffraction limit of classical optics[20,21] to yield information on even finer scale. However, in that case, crystalline anisotropy at the submicron scale may affect the relative intensities of the two peaks, and further calibration measurements may be required. Other problems that can be studied by laser micro-Raman could be secondary crystallization during spherulite annealing. Finally, the analysis presented here can also be applied to iPP/polymer blends to assess the crystallinity of the iPP domains as well as to iPP composites for which important issues such as the development of crystallinity at the vicinity of filler/fiber can be quantified at the microscale.

Acknowledgment. The financial support of both the General Secretariat for Research and Technology (GSRT) and the International Bureau of the German Federal Ministry for Education and Research (BMBF) at DLR (project; GRI-023-99) is gratefully acknowledged. C.M. gratefully acknowledges the Inter-Departmental Programme of Graduate Studies in Polymer Science and Technology for financial assistance.

References and Notes

(1) Miao, B.; Northwood, D. O.; Bian, W.; Fang, K.; Fan, M. H. *J. Mater. Sci.* **1994**, *29*, 255−260.
(2) Holzkey, G.; Muller, B. *Chem. Erde* **1999**, *59*, 183−189.
(3) Magill, J. H. *J. Mater. Sci.* **2001**, *36*, 3143−3164.
(4) Lehmann, O. *Molecularphysik*; Wilhelm Guglemann: Leipzig, 1888; Vol. 1.
(5) Karger-Kocsis, J. In *Polypropylene: An A-Z Reference*; Kluwer: Dordrecht, The Netherlands, 1999.
(6) D'Anielo, C.; Guadagno, L.; Gorrasi, G.; Vittoria, V. *Polymer* **2000**, *41*, 2515−2519.
(7) Karger-Kocsis, J.; Bárány, T. *Polym. Eng. Sci.* **2002**, *42*, 1410−1419.
(8) Varga, J. *J. Mater. Sci.* **1992**, *27*, 2557−2579.
(9) Lotz, B.; Wittmann, J. C.; Lovinger, A. J. *Polymer* **1996**, *37*, 4979−4992.
(10) Keith, H. D.; Padden, F. J.; Walter, N. M.; Wyckoff, H. W. *J. Appl. Phys.* **1959**, *30*, 1485−1488.
(11) Meille, S. V.; Ferro, D. R.; Brückner, S.; Lovinger, A. J.; Padden, F. J. *Macromolecules* **1994**, *27*, 2615−2622.
(12) Morrow, D. R.; Newman, B. A. *J. Appl. Phys.* **1968**, *39*, 4944−4950.
(13) McAllister, P. B.; Carter, T. J.; Hinde, R. M. *J. Polym. Sci., Polym. Phys.* **1978**, *16*, 49−57.
(14) Minogianni, C.; Gatos, K. G.; Galiotis, C. *Appl. Spectrosc.* **2005**, *59*, 1141−1147.
(15) Kellar, E. J. C.; Evans, A.; Galiotis, C.; Andrews, E. H. *Macromolecules* **1997**, *30*, 2400−2407.
(16) Kolb, R.; Wutz, C.; Stribeck, N.; von Krosig, G.; Riekel, C. *Polymer* **2001**, *42*, 5257−5266.
(17) Olley, R. H.; Bassett, D. C. *Polymer* **1982**, *23*, 1707−1710.
(18) Wu, C. M.; Chen, M.; Karger-Koscis, J. *Polym. Bull. (Berlin)* **1998**, *41*, 239−245.
(19) Van Haeringen, D. T.; Varga, J.; Ehrenstein, G. W.; Vancso, G. J. *J. Polym. Sci., Polym. Phys.* **2000**, *38*, 672−681.
(20) Betzig, E.; Trautman, J. K.; Harris, T. D.; Weiner, J. S.; Kostelac, R. L. *Science* **1991**, *251*, 1468−1470.
(21) Wang, J. J.; Smith, D. A.; Batchelder, D. N.; Saito, Y.; Kirkham, J.; Robinson, C.; Baldwin, K.; Li, G.; Bennett, B. *J. Microsc.* **2003**, *210*, 330−333.

MA0623284